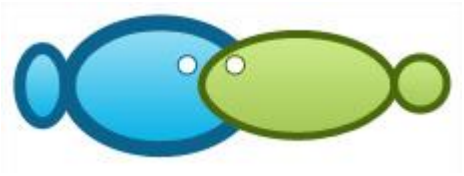

Hydroxyapatite/zeolite-based antibacterial composite derived from *Katsuwonus pelamis* bones and synthetic A-type zeolite

[1]Audy D. Wuntu, [2]Desy M. H. Mantiri, [2]James J. H. Paulus, [1]Henry F. Aritonang

[1] Chemistry Study Program, Faculty of Mathematics and Science, Sam Ratulangi University, Manado, Indonesia; [2] Marine Science Study Program, Faculty of Fisheries and Marine Science, Sam Ratulangi University, Manado, Indonesia. Corresponding author: A. D. Wuntu, wuntudenny@unsrat.ac.id

Abstract. The sea contains marine natural resources with a massive potential, including fish, which are mainly exploited to meet human food needs. Fish body parts such as bones, however, are often unused. The study was aimed to synthesize an antibacterial composite material based on hydroxyapatite (HAp) from skipjack tuna (*Katsuwonus pelamis*) bones and synthetic A-type zeolite (ZA). HAp was obtained from calcined fish bones and the mixtures of HAp/ZA in different ratios were prepared through a one-step procedure using silica gel and aluminum hydroxide as precursors for ZA. The antibacterial composite material was then obtained by reacting the mixture with silver nitrate ($AgNO_3$). The synthesized composite was characterized using X-ray diffractometry (XRD) and scanning electron microscope-energy dispersive X-ray (SEM-EDX). The antimicrobial activity of the composite was tested against Gram-positive *Staphylococcus aureus* and Gram-negative *Escherichia coli* bacteria. XRD characterization showed the presence of HAp, Ag-ZA, Ag_3PO_4 and Ag, and SEM-EDX confirmed the ZA in cubic shape and other particles in irregular-shaped granules. The antibacterial test showed that the best antibacterial activity against the two bacteria was exhibited by the composite having a HAp:ZA ratio of 1.5:1.
Key Words: skipjack tuna, Ag_3PO_4, Ag-zeolite, bacteria, inhibition zone.

Introduction. Oceans contain extraordinary quantities of still unused high quality natural resources of importance for the mankind welfare. Fish, a part of the marine biodiversity, is exploited on a large scale to meet various human needs. In the Fishbase database (Froese & Pauly 2019), it was noted that up to 2019, at least 34,300 species of marine and freshwater fish were identified in waters around the world, including skipjack tuna (*Katsuwonus pelamis*), which were mostly caught to fulfill human needs for food. Fish processing as food leaves out the bones, often wasted despite their hydroxyapatite (HAp) biomineral content, which has many uses. HAp generally contributes by up 60-70% to the weight of fish bones (Piccirillo et al 2013) and this mineral is easily extracted and exhibits biocompatibility with human bone tissue (Granito et al 2018). Studies were widely conducted in order to investigate the potential of HAp from fish bones as material for bone tissue engineering (Venkatesan et al 2011; Boutinguiza et al 2012; Venkatesan et al 2015; Piccirillo et al 2015; Yamamura et al 2018) and to provide enhanced biocompatible materials combining HAp with other substances such as zinc (Yang et al 2018), chitosan (Wikanta et al 2013), gelatin (Senthil et al 2018), wollastonite (Chen et al 2018), and ZSM zeolite (Iqbal et al 2016).

In the present study, a composite material based on HAp *K. pelamis* bones and A-type zeolite (ZA) was synthesized, and its ability to inhibit the growth of *Staphylococcus aureus* and *Escherichia coli* bacteria was examined to explore the potential of this composite as a biomedical material.

Material and Method. All the chemicals used were of analytical grade and deionized water was used for preparing the solutions in the experiment. 45 uniform size fresh *K.*

pelamis with a fork length of 30-40 cm were obtained in early July 2020 from a fish auction in Bitung, North Sulawesi, Indonesia. Subsequent work including composite synthesis and its characterization and antibacterial activity analysis was conducted in the next four months.

Fish bones preparation. The vertebrae were part of the bones used in this experiment. The bones were separated from the meat, boiled, cleaned of the still attached meat, air-dried for 24 hours, and then dried in an oven at 100^{o}C for 12 hours. The dried bones were then calcined at 1,000^{o}C for 5 hours to obtain HAp, which was then ground and sieved with a 100 mesh sieve.

Ag-treated HAp/ZA mixture. Silicate and aluminate solutions were adequately prepared by dissolving SiO_2 and $Al(OH)_3$, respectively, into NaOH 12 M solutions each. The two solutions were then mixed to initiate the formation of ZA and HAp was directly added to the solution. The amount of HAp added was adjusted to obtain mixtures of HAp and ZA having HAp:ZA mass ratio of 0.5:1, 1:1, and 1.5:1. The mixtures were then immediately heated in an oven at 90^{o}C for 4 hours, stirring periodically. After completion of heating, the existing precipitates were separated through filtering, rinsed with deionized water so that the pH of the filtrate becomes neutral, and then dried in an oven at 100^{o}C for 6 hours. The HAp/ZA mixtures were then reacted with $AgNO_3$ solution with a mole ratio of Ag:HAp=5:1, through stirring at 65^{o}C and 300 rpm for 24 hours. Subsequently, the mixtures were filtered, and the solids were heated in an oven at 90^{o}C for 6 hours. The obtained composites were characterized using X-ray diffractometry (XRD) (PanAnalytical E'xpertPro) to identify the crystalline phases present in the material and the XRD patterns were analyzed with reference the Crystallography Open Database (COD), using the Match!3 software. The composites were subsequently investigated according to the Rietveld refinement method, using the software, as well. A scanning electron microscope (SEM) (FEI Inspect-S50) equipped with energy dispersive X-ray (EDX) was also employed to explore the surface morphology and the elemental composition.

Antibacterial activity test. The antibacterial activity of the materials was tested against Gram-positive *S. aureus* and Gram-negative *E. coli* bacteria following the procedure described by Aritonang et al (2019). Distilled water and ciprofloxacin were used as negative and positive control, respectively. The diameter of the clear inhibition zone was measured using JMicroVision software.

Statistical analysis. Data of clear zone diameter reflecting the ability of the composites to inhibit bacterial growth with comparison to ciprofloxacin as positive control and distilled water as negative control were analyzed statistically using the Tukey test at the 95% confidence level.

Results and Discussion

XRD characterization. The XRD patterns of the composites are depicted in Figure 1 showing the existence of HAp, Ag-ZA (dehydrated), Ag_3PO_4 and Ag, which are compared to patterns from COD. HAp is the main biomineral component in fish bones, and its presence in the synthesized composites was confirmed by the diffraction peaks in terms of standard HAp (COD-ID 9002213). $AgNO_3$ treatment on the HAp/ZA mixtures resulted in Ag-ZA and Ag_3PO_4, which were identified by the diffraction peaks of standard Ag-ZA (COD-ID 4119066) and Ag_3PO_4 (COD-ID 2106404), respectively. The formation of Ag-ZA by ionic exchange of Ag^+ in the structure of ZA was shown by some researchers (Nosrati et al 2015; Bedi et al 2012; Cerrillo et al 2018). The formation of Ag_3PO_4 by treating fish bones with $AgNO_3$ was also demonstrated by Piccirilo et al (2014) using cod fish bones treated with the chemical before calcination. In our work, it was demonstrated that Ag_3PO_4 could also be generated from *K. pelamis* bones employing a slightly different method involving $AgNO_3$ treatment on the calcined bones. The components' relative

weight (%) in the composites was estimated by using the Rietveld refinement method, as shown in Table 1. The increasing HAp and the decreasing ZA were in line with the elevation of the HAp:ZA ratio. The increasing Ag_3PO_4 in the composites was also consistent with the increasing amount of precursor $AgNO_3$ accompanying the increased ratio of HAp:ZA. On the other hand, the presence of Ag, referring to standard Ag (COD-ID 1509145), was found in a small amount because it was consumed in the formation of Ag-ZA and Ag_3PO_4.

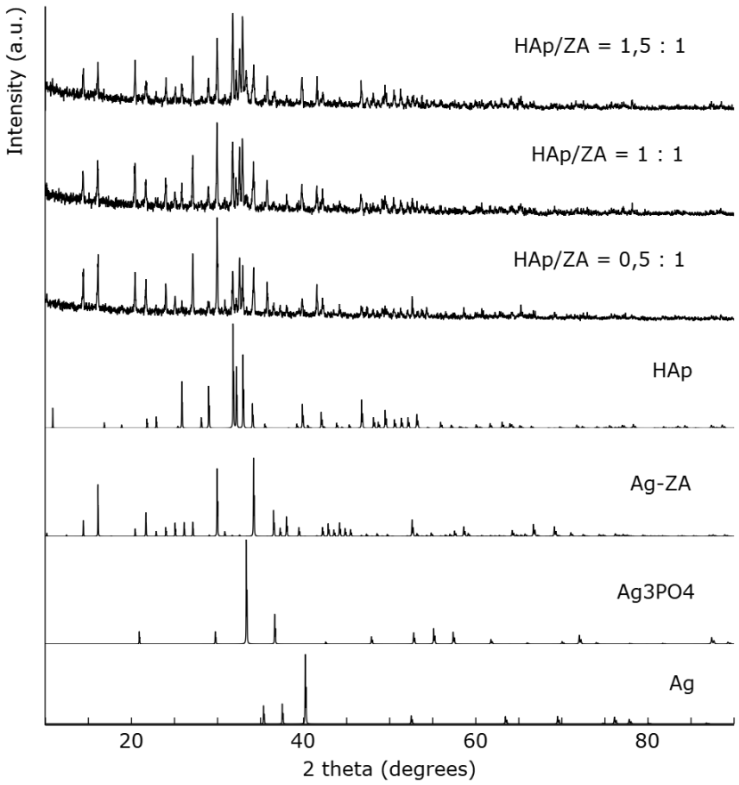

Figure 1. XRD patterns for the synthesized composites and comparison with the standard diffraction patterns for HAp, Ag-ZA, Ag_3PO_4, and Ag.

Table 1
Composition (% weight) of the composites estimated by the Rietveld refinement method

Component	*HAp:ZA=0.5:1*	*HAp:ZA=1:1*	*HAp:ZA=1.5:1*
HAp	56.9	65.3	71.8
Ag-ZA	41.5	31.1	22.8
Ag_3PO_4	0.4	2.2	4.6
Ag	1.2	1.4	0.8

Morphlogy and elemental composition. The morphology of the composite particles analyzed by SEM is shown in Figure 2. Careful observation of the morphology of the composites clearly revealed the presence of Ag-ZA in cube-shaped particles which are typical of ZA, most of them sizing 0.5-1.5 μm. This cubic shape was also observed by Cerrillo et al (2018) on Ag-ZA synthesized using commercial ZA. Other particles observed were smaller spherical grains consisting of HAp and Ag_3PO_4 particles. Piccirillo et al (2014) showed that HAp particles are larger and could be distinguished from smaller Ag_3PO_4. Metallic silver might exist as nanoparticles, below the resolution of SEM technique, and in amounts so small that it was not observed. The presence of more spherical grains with increasing HAp: ZA ratio was a response to the increase of the HAp added and to the increase of the Ag_3PO_4 formed. The tendency of increased HAp concentrations could also be noted from the elemental analysis (% weight) of the

composites using EDX (Table 2). The increase in the HAp concentrations with the HAp:ZA ratio was revealed by the increase in the concentrations of P and Ca. On the other hand, the sodium in the ZA structure appeared to be completely removed by Ag^+ via a cation exchange to produce Ag-ZA.

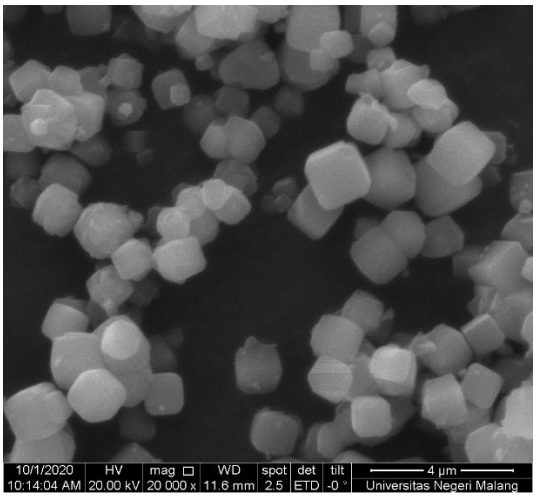

(a)

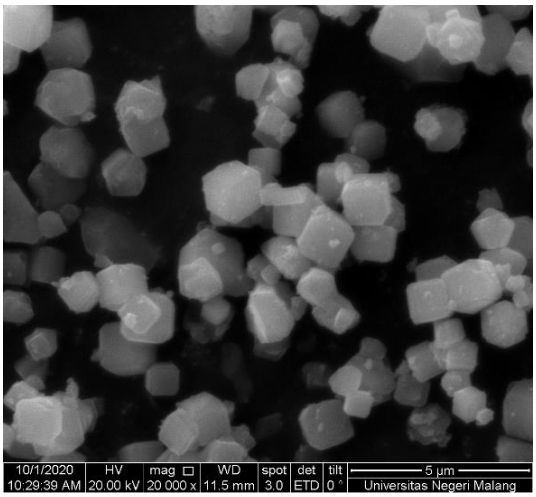

(b)

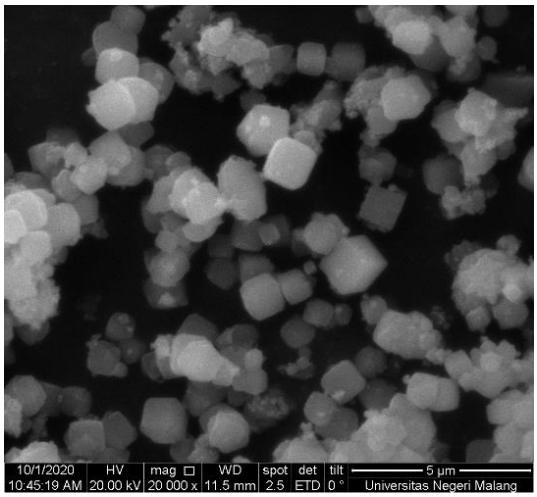

(c)

Figure 2. SEM images of Ag-treated HAp/ZA-based composites. (a) HAp:ZA=0.5:1, (b) HAp:ZA=1:1, (c) HAp:ZA=1.5:1.

Table 2

Elemental composition (% weight) of the composites analyzed using EDX

Element	*HAp:ZA=0.5:1*	*HAp:ZA=1:1*	*HAp:ZA=1.5:1*
O	29.51	32.97	31.47
Na	2.16	0.00	0.33
Al	11.33	9.41	8.00
Si	9.84	7.81	7.44
P	1.99	3.96	5.69
Ag	40.59	37.90	36.71
Ca	4.58	7.95	10.37

Antibacterial activity. The antibacterial test by measuring the diameter of the clear zones, around the wells containing the synthesized antibacterial composites, showed that these composites had the potential as an antibacterial material against Gram-positive *S. aureus* and Gram-negative *E. coli* bacteria (Figure 3). The distinct zones around the wells

containing the compounds ciprofloxacin (as a positive control) and distilled water (as a negative control) reflect the ability of antibacterial agents to inhibit bacterial growth. It was obvious that the zones were only formed around the wells containing the antibiotic ciprofloxacin and the materials synthesized in this study, but not around the wells containing the dispersing agent (distilled water). The diameter of the inhibition zone formed around these wells is shown in Table 3.

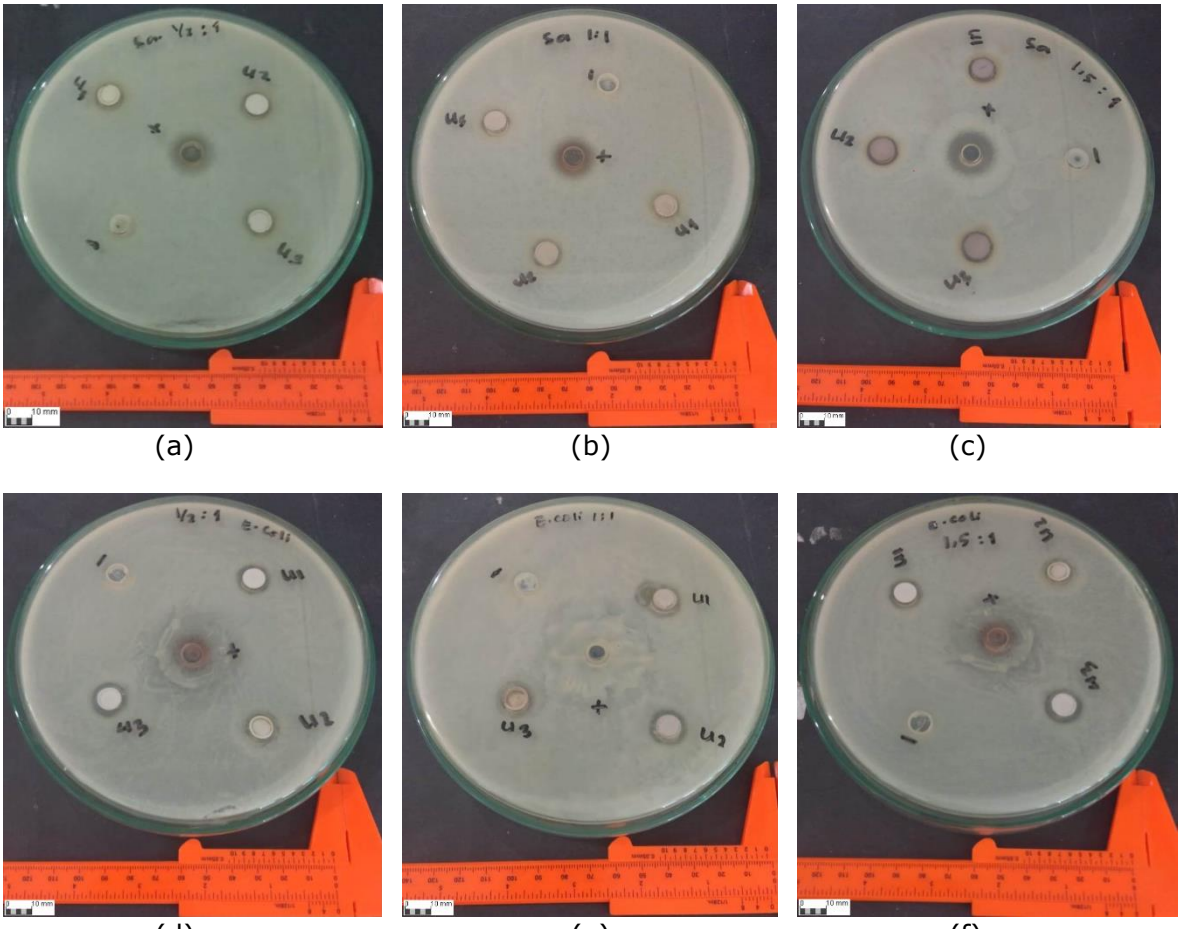

(a) (b) (c)

(d) (e) (f)

Figure 3. Antibacterial activity of (a) HAp:ZA=0.5:1, (b) HAp:ZA=1:1, (c) HAp:ZA=1.5:1 against *Staphylococcus aureus* and (d) HAp:ZA=0.5:1, (e) HAp:ZA=1:1, (f) HAp:ZA=1.5:1 against *Escherichia coli.*

Table 3

Diameter (mm) of the inhibition zone

Bacteria	*Replication*	*Negative control*	*HAp:ZA= 0.5:1*	*HAp:ZA= 1:1*	*HAp:ZA= 1.5:1*	*Positive control*
Staphylococcus aureus	1	0	10.68	11.92	11.66	17.43
	2	0	10.81	12.83	13.12	17.26
	3	0	11.62	11.92	13.85	18.54
	Mean	0^{a}	11.04^{b}	$12.22^{b,c}$	12.88^{c}	17.74^{d}
Escherichia coli	1	0	12.34	13.08	13.56	14.68
	2	0	12.66	14.47	12.67	14.78
	3	0	13.09	13.51	15	15.44
	Mean	0^{f}	12.70^{g}	$13.69^{g,h}$	$13.74^{g,h}$	14.97^{h}

Values indicated with the different letters shows significant difference at the 95% confidence level.

Table 3 shows that the composites had an antibacterial activity. Those with the ratios of HAp:ZA=1:1 and HAp:ZA=1.5:1 gave the best results and were not significantly different

from the ciprofloxacin's antibacterial activity against *E. coli* bacteria. On the other hand, the antibacterial activity of the composites with the HAp:ZA ratios of 1:1 and 1:1.5 were not significantly different, although their activity was significantly lower than the antibacterial activity of ciprofloxacin against *S. aureus* bacteria. The metallic Ag, despite its small concentration in the composites, was very effective as antibacterial agent (Junping et al 2015), but the Ag_3PO_4 and Ag-ZA had the main contribution to the bacterial inhibition. It was shown by Wu et al (2013) that Ag_3PO_4 could have antibacterial activity against *E. coli* bacteria. The antibacterial activity of Ag_3PO_4 involved the release of Ag^+ ions from Ag_3PO_4, which then attacked the bacteria. Another study by Cerrillo et al (2018) showed that Ag-ZA was also a material that had the ability to inhibit the growth of *S. aureus* and *E. coli* bacteria. The antibacterial mechanism of this material was also preceded by the release of Ag^+, but it was not fully understood (Yang & Hu 2015), a study by Feng et al (2000) suggesting that Ag^+ caused DNA molecules to condense so that the bacteria lose their ability to replicate. Besides, Ag^+ ions could interact with thiol groups in bacterial proteins, inactivating them. Jung et al (2008) showed that Ag^+ entering the media could interfere with the mechanism required by the bacteria in the uptake and utilization of substrates for cell division, causing the shrinkage of the cytoplasmic membrane and the separation of the cell wall, which determined the outward diffusion of the cellular content and the subsequent cellular death. While the composites synthesized in this study were more effective in inhibiting the growth of *E. coli* bacteria, the ciprofloxacin, in contrast, showed a better antibacterial activity against *S. aureus* (Table 3). Similar results were found by previous researchers (Cerrillo et al 2018; Siddiqui et al 2013; Jung et al 2008) who suggested that the antibacterial effectiveness was related to the structure of the bacterial cell wall.

Conclusions. Antibacterial composites containing HAp, Ag-ZA, Ag_3PO_4, and Ag could be synthesized from HAp derived from *K. pelamis* bones and synthetic ZA. The synthesis procedure by direct application of $AgNO_3$ on mixtures containing HAp (from calcined *K. pelamis* bones) and synthetic ZA resulted in Ag_3PO_4 and Ag-ZA (via Na substitution). The composite with a HAp/ZA ratio of 1.5:1 exhibited the best antibacterial activity. The performance, however, was not significantly different from that of the composite with a HAp/ZA ratio of 1:1 against *S. aureus* and *E. coli* bacteria.

Conflict of interest. The authors declare no conflict of interest.

References

Aritonang F. A., Koleangan H., Wuntu A. D., 2019 Synthesis of silver nanoparticles using aqueous extract of medicinal plants' (*Impatiens balsamina* and *Lantana camara*) fresh leaves and analysis of antimicrobial activity. International Journal of Microbiology 8642303, https://doi.org/10.1155/2019/8642303.

Bedi R. S., Cai R., O'Neill C., Beving D. E., Foster S., Guthrie S., Chen W., Yan Y., 2012 Hydrophilic and antimicrobial Ag-exchanged zeolite A coatings: A year-long durability study and preliminary evidence for their general microbiocidal efficacy to bacteria, fungus and yeast. Microporous and Mesoporous Materials 151:352-357.

Boutinguiza M., Pou J., Comesaña R., Lusquiños F., de Carlos A., León B., 2012 Biological hydroxyapatite obtained from fish bones. Materials Science and Engineering 32:478-486.

Cerrillo J. L., Palomares A. E., Rey F., Valencia S., Perez-Gago M. B., Villamon D., Palou L., 2018 Functional Ag-exchanged zeolites as biocide agents. Chemistry Select 3:4676-4682.

Chen Z., Zhai J., Wang D., Chen C., 2018 Bioactivity of hydroxyapatite/wollastonite composite films deposited by pulsed laser. Ceramics International 44(9):10204-10209.

Feng Q. L., Wu J., Chen G. Q., Cui F. Z., Kim T. N., Kim J. O., 2000 A mechanistic study of the antibacterial effect of silver ions on *Escherichia coli* and *Staphylococcus aureus*. Journal of Biomedical Materials Research 52(4):662-668.

Froese R., Pauly D., 2019 FishBase: World Wide Web electronic publication. www.fishbase.org
Granito R. N., Renno A. C. M., Yamamura H., de Almeida M. C., Ruiz P. L. M., Ribeiro D. A., 2018 Hydroxyapatite from fish for bone tissue engineering: A promising approach. International Journal of Molecular and Cellular Medicine 7(2):80-90.
Iqbal N., Kadir M. R. A., Iqbal S., Razak S. I. A., Rafique M. S., Bakhsheshi-Radd H. R., Idris M. H., Khattake M. A., Raghavendranf H. R. B., Abbas A. A., 2016 Nano-hydroxyapatite reinforced zeolite ZSM composites: A comprehensive study on the structural and in vitro biological properties. Ceramics International 42(6):7175-7182.
Jung W. K., Koo H. C., Kim K. W., Shin S., Kim S. H., Park Y. H., 2008 Antibacterial activity and mechanism of action of the silver ion in *Staphylococcus aureus* and *Escherichia coli*. Applied and Environmental Microbiology 74(7):2171-2178.
Junping Y., Yuheng H., Lingxia C., 2015 Research and development of antibacterial metallic materials. Proceedings of the International Conference on Chemical, Material and Food Engineering, Atlantis Press, Amsterdam, pp. 51-54.
Nosrati R., Olad A., Nofouzi K., 2015 A self-cleaning coating based on commercial grade polyacrylic latex modified by TiO_2/Ag-exchanged-zeolite-A nanocomposite. Applied Surface Science 346:543-553.
Piccirillo C., Pintado M. M., Castro P. M. L., 2013 Hydroxyapatite and calcium phosphates from marine sources: extraction and characterization. In: Marine biomaterials: characterization, usolation, and applications. Kim S-K. (ed), pp. 29-44, CRC Press, Taylor & Francis Group.
Piccirillo C., Pinto R. A., Tobaldi D. M., Pullar R. C., Labrincha J. A., Pintado M. M. E., Castro P. M. L., 2014 Light induced antibacterial activity and photocatalytic properties of Ag/Ag_3PO_4-based material of marine origin. Journal of Photochemistry and Photobiology A: Chemistry 296:40-47.
Piccirillo C., Pullar R. C., Costa E., Santos-Silva A., Pintado M. M. E., Castro P. M. L., 2015 Hydroxyapatite-based materials of marine origin: a bioactivity and sintering study. Materials Science and Engineering C 51:309-315.
Senthil R., Vedakumari S. W., Sastry T. P., 2018 Hydroxyapatite and demineralized bone matrix from marine food waste - a possible bone implant. American Journal of Materials Synthesis and Processing 3(1):1-6.
Siddiqui T., Naqvi B. S., Alam N., Bashir L., Naz S., Naqvi G., Baig M. T., Tasleem S., 2013 Antimicrobial susceptibility testing of ciprofloxacin & cefepime against *Staphylococcus aureus* & *Escherichia coli*. International Journal of Scientific & Engineering Research 4(12):1386-1389.
Venkatesan J., Qian Z. J., Ryu B., Thomas N. V., Kim S.-K., 2011 A comparative study of thermal calcination and an alkaline hydrolysis method in the isolation of hydroxyapatite from *Thunnus obesus* bone. Biomedical Materials 6(3):035003, https://doi.org/10.1088/1748-6041/6/3/035003.
Venkatesan J., Lowe B., Manivasagan P., Kang K.-H., Chalisserry E. P., Anil S., Kim D. G., Kim S.-K., 2015 Isolation and characterization of nano-hydroxyapatite from salmon fish bone. Materials 8(8):5426-5439.
Wikanta T., Erizal, Sugiyono, 2013 Chitosan composite of crab shell and hydroxyapatite of tuna fish bone as biomaterials for guided tissue regeneration. Squalen Bulletin of Marine and Fisheries Postharvest and Biotechnology 8(3):95-104.
Wu A., Tian C., Chang W., Hong Y., Zhang Q., Qu Y., Fu H., 2013 Morphology-controlled synthesis of Ag_3PO_4 nano/microcrystals and their antibacterial properties. Materials Research Bulletin 48:3043-3048.
Yamamura H., da Silva V. H. P., Ruiz P. L. M., Ussui V., Lazar D. R. R., Renno A. C. M., Ribeiro D. A., 2018 Physico-chemical characterization and biocompatibility of hydroxyapatite derived from fish waste. Journal of Mechanical Behavior of Biomedical Materials 80:137-142.
Yang H., Qu X., Lin W., Wang C., Zhu D., Dai K., Zheng Y., 2018 In vitro and in vivo studies on zinc-hydroxyapatite composites as novel biodegradable metal matrix composite for orthopedic applications. Acta Biomaterialia 71:200-214.

Yang Y., Hu H., 2015 A review on antimicrobial silver absorbent wound dressings applied to exuding wounds. Journal of Microbial & Biochemical Technology 7(4):228-233.

Received: 01 January 2021. Accepted: 18 February 2021. Published online: 28 February 2021.
Authors:
Audy Denny Wuntu, Sam Ratulangi University, Faculty of Mathematics and Science, Chemistry Study Program, Jalan Kampus Unsrat Bahu Manado 95115, Indonesia, e-mail: wuntudenny@unsrat.ac.id
Desy Maria Helena Mantiri, Sam Ratulangi University, Faculty of Fisheries and Marine Science, Marine Science Study Program, Jalan Kampus Unsrat Bahu Manado 95115, Indonesia, e-mail: dhm_mantiri@unsrat.ac.id
James Jobert Hanoch Paulus, Sam Ratulangi University, Faculty of Fisheries and Marine Science,Marine Science Study Program, Jalan Kampus Unsrat bahu Manado 95115, Indonesia, e-mail: jamespaulus@unsrat.ac.id
Henry Fonda Aritonang, Sam Ratulangi University, Faculty of Mathematics and Science,Chemistry Study Program, Jalan Kampus Unsrat Bahu Manado 95115, Indonesia, e-mail: henryaritonang@unsrat.ac.id

How to cite this article:
Wuntu A. D., Mantiri D. M. H., Paulus J. J. H., Aritonang H. F., 2021 Hydroxyapatite/zeolite-based antibacterial composite derived from *Katsuwonus pelamis* bones and synthetic A-type zeolite. AACL Bioflux 14(1):612-619.